



Published in final edited form as:

Nat Commun. 2013 ; 4: 2149. doi:10.1038/ncomms3149.

Autonomous Vascular Networks Synchronize GABA Neuron Migration in the Embryonic Forebrain

Chungkil Won¹, Zhicheng Lin², Peeyush Kumar T¹, Suyan Li¹, Lai Ding³, Abdallah Elkhal⁴, Gábor Szabó⁵, and Anju Vasudevan^{1,φ}

¹Department of Psychiatry, Harvard Medical School, Boston, MA; and Angiogenesis and Brain Development Laboratory, Division of Basic Neuroscience, McLean Hospital, 115 Mill Street, Belmont, MA-02478, USA

²Department of Psychiatry, Harvard Medical School, Boston, MA; and Division of Alcohol and Drug Abuse, McLean Hospital, 115 Mill Street, Belmont, MA-02478, USA

³Enhanced Neuroimaging Core, Harvard NeuroDiscovery Center, Harvard Medical School, Goldenson Building 501, 220 Longwood Avenue, Boston, MA-02115, USA

⁴Department of Surgery, Harvard Medical School, Boston, MA; and Division of Transplantation, Brigham and Women's Hospital, 221 Longwood Avenue, EBRC 309, Boston, MA-02115, USA

⁵Institute of Experimental Medicine, Department of Gene Technology and Developmental Neurobiology, Laboratory of Molecular Biology and Genetics, 1083 Budapest, Hungary

Abstract

GABA neurons, born in remote germinative zones in the ventral forebrain (telencephalon), migrate tangentially in two spatially distinct streams to adopt their specific positions in the developing cortex. The cell types and molecular cues that regulate this divided migratory route remains to be elucidated. Here we show that embryonic vascular networks are strategically positioned to fulfill the task of providing support as well as critical guidance cues that regulate the divided migratory routes of GABA neurons in the telencephalon. Interestingly, endothelial cells of the telencephalon are not homogeneous in their gene expression profiles. Endothelial cells of the periventricular vascular network have molecular identities distinct from those of the pial network. Our data suggest that periventricular endothelial cells have intrinsic programs that can significantly mold neuronal development and uncovers new insights into concepts and mechanisms of CNS angiogenesis from both developmental and disease perspectives.

Users may view, print, copy, download and text and data- mine the content in such documents, for the purposes of academic research, subject always to the full Conditions of use: http://www.nature.com/authors/editorial_policies/license.html#terms

^φ Correspondence should be addressed to: A.V. (avasudevan@mclean.harvard.edu).

Author Contributions: AV designed the study; CW, PKT and SL performed dissections, culture experiments, immunostainings and imaging; ZL conducted gene expression profile analysis; LD assisted with confocal microscopy and performed ImageJ analysis; AE conducted FACS and ELISA; GS provided the GAD65-GFP line and comments on the manuscript; AV supervised all phases of the project, analyzed data, prepared figures and wrote the manuscript.

Competing interests statement: The authors declare no competing financial interests.

Introduction

Abnormalities in GABA neurons are implicated as a major factor in many neurological disorders ranging from epilepsy to autism and schizophrenia¹⁻⁴. Whether this occurs by developmental and/or degenerative processes, abnormalities in neurons and their synapses usually receive prime consideration. However, when the key to complete understanding of the complicated pathophysiology as in the case of schizophrenia and finding solutions to successful therapy continues to elude us now for more than a century, it becomes critical to approach this problem with new perspectives. Our studies have shown the significance of the other cell type –“endothelial cells” in the embryonic forebrain and challenged notions of cerebral vascularization that imply that blood vessels sprout passively into the brain parenchyma from pial vascular plexuses to meet metabolic needs of growing neuronal populations^{5, 6}. Based on anatomical location, independent growth patterns and developmental regulation, telencephalic blood vessels fall into two categories: pial and periventricular. While the neural tube directs the formation of the pial vessels that envelop it by embryonic day 9 (E9)⁷, the periventricular vessels originate from a basal vessel on the telencephalic floor of the basal ganglia primordium and develop in an orderly, ventral-to-dorsal gradient by E11^{5, 6}.

The direction of the periventricular endothelial cell gradient matches the direction of GABA neuron migration from the basal to the dorsal telencephalon but with respect to timing, the angiogenesis gradient is in advance by about a day. GABA neurons on their tangential journey to the dorsal telencephalon arrive at the pallial-subpallial boundary (PSB) at E12 (Reference⁸ and Supplementary Fig. S1). Not only did the timing of this migration seem striking in comparison with the prior migration of endothelial cells of the periventricular network, but also the periventricular endothelial cells and GABA neurons follow the same migratory route. At E13, the distribution of GABA neurons into two spatially distinct streams in the dorsal telencephalon, a slender stream in the marginal zone (MZ) that is close to the pial network and another broader stream in the subventricular (SVZ) zone in the route of periventricular vessel gradient seemed very intriguing. The origins and routes of tangential migration of telencephalic GABA neurons are well-established⁹⁻¹¹. However, many missing links remain and the mechanisms that underlie GABA neuron tangential migration are not fully understood. Although, elegant work has demonstrated diverse modes of migration in the CNS, like radial-glia dependent neuronal migration^{12, 13} and homophilic migration of the cells of the RMS¹⁴, the mode of migration of telencephalic GABA neurons has yet to be identified. For some time, it was speculated that GABA interneurons used the cortical-fugal fibers in the IZ as a guide^{15, 16} until it was conclusively ruled out¹⁷. The existing cortical radial glial scaffold was also presumed to act as a guide for GABA interneurons when they enter the cortical plate¹⁰, however, no such glial guides are present when the GABA cells migrate out of the ventral telencephalon. The most widely accepted model for GABA neuron migration suggests that migration is dictated by the simultaneous activity of chemorepulsive and chemoattractive gradients¹⁸⁻²⁰. Several families of ligands/receptors (Slit/Robo, semaphorin/neuropilin, Neuregulin-1/ErbB4²¹⁻²⁴), motogenic factors (HGF, SDF1/CXCL12), GDNF and BDNF^{20, 25-29} as well as projection neuron precursors in the IZ-SVZ via CXCL12/CXCR4 signaling³⁰ have been proposed as candidates for

guiding trajectories of GABA neurons. Nevertheless, key aspects into how exactly these factors influence formation and segregation of GABA neurons into a dual stream and direct them from the basal forebrain into the developing cortex remain undetermined and in this regard the enigma of GABA neuron tangential journey has remained elusive.

Here we elucidate several new concepts about autonomy in embryonic vascular networks that regulate GABA neuron migration in the mouse telencephalon at an early embryonic stage, E13. We show that endothelial cells from the periventricular network are distinct from those of the pial network with remarkable versatility in being able to co-ordinate neuronal development.

Results

GABA neurons are closely associated with vascular networks

From current literature^{8, 10, 17} and from Supplementary Fig. S1, the spatially distinct GABA neuron streams of the MZ and SVZ are obvious, but the telencephalic location, whether it is at the PSB or in the subpallium that GABA neurons segregate to form these dual streams was unclear to us. Vibratome sections of E13 GAD65-GFP telencephalon were labeled with blood vessel marker, isolectin B4 at all rostral-caudal levels. Our observations reveal that formation of the dual GABA stream occurs deep within the ventral telencephalon. Indeed, GABA neurons can be visualized splitting into two streams in the ventral telencephalon and each stream enters one of two corridors created by the pial and periventricular networks (Fig. 1a–j). Confocal Z-stack images show us how the deep stream of GABA neurons taking this curved route are aligned with the periventricular vessel network. The rhombic vascular patterns ensheath deep GABA neurons in a tube-like form (Fig. 1c–j). GABA neurons that segregate from the deep stream form the narrow superficial stream next to the pial network (Fig. 1d–g). The profile of periventricular vessels associated with the deep GABA neuron stream is directed tangentially towards the PSB (Fig. 1a, b). Periventricular vessels approaching the PSB have a slightly curved profile that extends into the pallium (Fig. 1k, Supplementary Fig. S1). Periventricular vessels in the ganglionic eminence (GE) form a continuous tube-like plexus that connect to the vessels near the PSB (Fig. 1k). GABA neurons of the deep stream (Fig. 1c–j) and from the ganglionic eminence (Fig. 1l) adhere closely to their respective periventricular vascular profiles that lead them near the PSB where they form a single uniform stream (Fig. 1l). The profile of periventricular vessels near and around the PSB is very unique since it herds the GABA neuron stream uniformly into the SVZ of the dorsal telencephalon (Fig. 1k, l, Supplementary Fig. S1). This arrangement of periventricular vessel network in the ventral telencephalon that supports GABA neuron migration towards the PSB was observed in E13 slices at both rostral (Fig. 1a–l) and caudal levels (Fig. 1m, n). The lattice arrangement of periventricular vessels at the PSB (Fig. 1o) continues into the SVZ region of the dorsal telencephalon (Fig. 1p) where the deep stream of GABA neurons migrate (Fig. 1q, Supplementary Fig. S1). We found a close physical association between the periventricular vascular network and deep stream of GABA neurons in both ventral and dorsal telencephalon (Fig. 1a–t, Supplementary Fig. S1). This intimate vessel-GABA neuron contact was recapitulated in forebrain sections from E13 CD1 mice that were labeled with isolectin B4 and GAD65/GAD67 markers. High magnification

images captured from ventral and dorsal telencephalon show processes of GABA neurons wrapped around individual periventricular vessels (Fig. 1u, v). We quantified the association of vasculature associated deep seated GABA neurons in the telencephalon and found that nearly 84% of randomly selected GFP+ve cells were located within 5 μ m of periventricular vessels (Fig. 1w). Interestingly, in the absence of a pre-formed periventricular vascular network in the dorsal telencephalon, GABA neurons from the ventral telencephalon failed to enter into the dorsal telencephalon (Supplementary Fig. S2).

Chemoattractive responses of GABA neurons are selective

Given the formation of the dual GABA neuron stream in the ventral telencephalon and the close association of either stream with pial and periventricular vascular networks, it seemed inevitable that pial versus periventricular endothelial cell cues act in bringing about this segregation. We considered whether GABA neurons acquired information about their migration trajectories from guidance cues that they encountered in the endothelial cells *en route*.

To answer these questions, our strategy was to present explants that derive GABA neurons of the deep stream and explants that derive GABA neurons of the superficial stream with a choice of periventricular endothelial cells (pv ecs) on one side and pial endothelial cells (pial ecs) on the other. Pial membranes were removed from intact telencephalon of E13 CD1 embryos by mechanical peeling and endothelial cells were isolated (Fig. 2a). The telencephalon without pial membranes was used to isolate periventricular endothelial cells (Fig. 2a). Cultures of pial and periventricular endothelial cells were thus prepared. We inserted culture inserts into the center of 35mm collagen coated culture dishes to create a barrier and plated periventricular endothelial cells on one side and pial endothelial cells on the other (Fig. 2b). Cells were allowed to grow to confluence on either side of the barrier. The barrier was removed just at the start of the endothelial cell - GABA neuron co-culture experiment. Endothelial cells seated at the border at this stage could be observed forming a single line with no migration into the area that had been occupied by the barrier (Fig. 2b). Slice preparations of E13 GAD65-GFP brains were made and two explants were dissected out: 1) sub-cortical telencephalon containing ganglionic eminence (GE) and 2) sub-pial surface of ventral telencephalon (sps). Explants were placed in the center of the endothelial cell-free area of culture dishes (Fig. 2c, d). This experimental design allowed us to sufficiently test chemoattractive activity of the deep and superficial set of GABA neurons when confronted with a choice of periventricular or pial endothelial cells. Interestingly, GE explants were markedly attracted towards periventricular endothelial cells and showed little response to pial endothelial cells (Fig. 2e, g, h). An interesting observation was that a significant number of periventricular endothelial cells lodged at the border at the start of the experiment crossed over and migrated towards the GE explant (Fig. 2f). A unique characteristic of periventricular endothelial cells is their robust migratory capacity when compared to pial ecs (Fig. 2f, i). On the other hand, sps explants showed significant chemotactic response to pial endothelial cells and minor response to periventricular endothelial cells (Fig. 2j, l, m). Although many periventricular endothelial cells migrated towards the explant (Fig. 2k), minimal response was seen on the part of the sps explant towards these endothelial cells (Fig. 2l). Co-labeled images of the chemoattractive response

of GE and sps derived GABA neurons towards periventricular and pial endothelial cells are also shown (Fig. 2o–r). The chemoattractive response of GE and sps explants towards periventricular and pial endothelial cells were quantified (Fig. 2s, t). The results of this experiment have been summarized in the schema (Fig. 2u, v). This experiment demonstrates that GABA neurons of the deep and superficial streams respond selectively to chemoattractive cues secreted by periventricular and pial endothelial cells.

Endothelial cells selectively guide GABA neuron migration

To test if distinct endothelial cells could specifically influence the migration of GABA neurons, we evaluated the migration of deep and superficial sets of GABA neurons from GE and sps explants on thin layers of basement membrane (BM) matrices that was seeded with either periventricular, pial or control endothelial cells (Fig. 3a–i). Control endothelial cells were prepared from other embryonic brain regions (E13 mesencephalon and metencephalon combined). GE explants showed significantly more robust migration on matrices seeded with periventricular endothelial cells, both in terms of cell number and migratory distance when compared to explants cultured on matrices seeded with pial or control endothelial cells (Fig. 3b–e). Sps explants, on the other hand migrated significantly on matrices seeded with pial endothelial cells when compared to periventricular or control endothelial cells (Fig. 3f–i). The controls (Fig. 3d, h) confirm that the effects on cell migration from GE and sps explants are specific for periventricular endothelial cells and pial endothelial cells (Fig. 3b–i). Since the BM matrix itself might be a conducive substrate for migration, we cultured our explants on a bed of pial, periventricular or control endothelial cells alone. Our results were similar to those obtained on BM matrices. GABA neurons from sps explants migrated well only on pial endothelial cells (Fig. 3j) and GABA neurons from GE explants migrated extensively only on periventricular endothelial cells (Fig. 3k). In some of our culture dishes, periventricular endothelial cells formed lattice patterns and the close association of migrating GABA neurons to these endothelial cells closely resembled the *in vivo* situation (Fig. 3l). Even within six hours, GABA neurons from the GE explants were seen taking a migratory route in close association to periventricular endothelial cells (Fig. 3m–o). These results show that periventricular endothelial cells selectively promote migration of the deep GABA neuron population while pial endothelial cells promote migration of the superficial GABA neuron population.

To study the importance of either vascular network for the formation of deep and superficial GABA neuron streams, we selectively disrupted either the periventricular vessel gradient (Fig. 3p–r) or the pial network (Fig. 3s–u). Cultures of intact E12 GAD65-GFP telencephalon were prepared (the stage when GABA neurons have just arrived at the PSB) and beads treated with angiogenesis inhibitor TNP-470, a fumagillin derivative^{31, 32}, were placed along the ventricular zone of the dorsal telencephalon. By this method, we were able to disrupt the periventricular vessel gradient selectively while the pial network was unaffected (Fig. 3q). The concentration of angiogenesis inhibitor used in this experiment does not cause cell death of cultured GABA neurons or affect migration from explant cultures (Supplementary Fig. S3). Control explants received beads treated with PBS and showed normal formation of periventricular and pial networks and the dual streams of GABA neurons (Fig. 3p). Interestingly, in the absence of a normal periventricular vessel

network, formation of the deep stream in the SVZ was significantly affected while the superficial stream in the MZ formed adjacent to the pial network (Fig. 3q). Since meningeal cells rapidly degenerate upon exposure to 6-hydroxydopamine⁵, we exposed E12 GAD65-GFP telencephalic explants to 6-hydroxydopamine. In explants treated with 6-hydroxydopamine, although pial network was disrupted, periventricular vessels were unaffected (Fig. 3t). Disruption of the pial network significantly disturbed superficial stream formation in the MZ (Fig. 3t) when compared to the respective control (Fig. 3s) while the deep stream of GABA neurons formed normally in the SVZ (Fig. 3s, t). The reduction in mean density of GABA neurons of the SVZ (Fig. 3p, q) and MZ (Fig. 3s, t) streams were quantified. Collectively these data point to a novel role for pial and periventricular vascular networks in instructing and promoting the selective migration of GABA neurons as two distinct streams in the early embryonic telencephalon.

Unique gene expression in periventricular endothelial cells

Since pial and periventricular endothelial cells were independently capable of acting as substrates and providing distinct guidance cues to aid migration of the individual GABA neuron streams, we reasoned that the outcome of gene expression profiles of pial endothelial cells and periventricular endothelial cells would be distinct. To address this question, endothelial cells from pial, periventricular and control (mesencephalon and metencephalon combined) samples obtained from E13 Tie2-GFP mice (in which endothelial cells express GFP) were stringently sorted by dual FACS analysis (with an endothelial cell marker, CD-31) to obtain pure populations of pial, periventricular and control endothelial cells respectively (Fig. 4a). RNA was extracted from all samples and subsequent microarray hybridization and analysis were performed.

This resulted in 2,426 genes upregulated in periventricular endothelial cells and 1567 genes downregulated when compared to pial endothelial cells. To examine the overall differences in expression closely, genes were classified into forty five functional categories (Fig. 4b). Interestingly, periventricular endothelial cells showed increased expression in genes that are specific to the central theme of embryonic forebrain development like neurogenesis, differentiation, morphogenesis, migration, chemotaxis and axon guidance when compared to pial endothelial cells. We screened for pathways and processes that were over- or under-represented in one endothelial cell type with respect to the other (Supplementary Figures S4–S11). Gene expressions for biological processes and canonical maps containing genes controlling neuronal development, cell proliferation, cell migration and immune response were enriched in periventricular endothelial cells (Supplementary Figures S4–S7). Gene expressions for endothelial cell contacts by non-junctional mechanisms, chemokines and cell adhesion as well as extracellular matrix remodelling were comparable in pial versus periventricular endothelial cells (Supplementary Figures S8–S10).

We next classified the genes according to disease categories and made another key discovery. The genes expressed in periventricular endothelial cells were enriched in disease categories like schizophrenia, nervous system diseases, epilepsy, autism, mood and depressive disorders (Fig. 4c and Fig. 5a), whereas those in pial endothelial cells were enriched in inflammation and pathological process categories (Fig. 5a). Independent repeats

of microarray hybridization and analysis performed with control endothelial cells and telencephalic periventricular endothelial cells showed similar results. The genes expressed in periventricular endothelial cells remained consistently enriched in disease categories like schizophrenia, psychiatric diseases, nervous system diseases, epilepsies, autism, bipolar, mood and depressive disorders when compared to control endothelial cells (Fig. 5b). The genes expressed in control endothelial cells were enriched in disease categories that were non neuro-psychiatric (Fig. 5b). This gene expression profile with enrichment of several neuro-psychiatric disease categories is thus a unique characteristic of periventricular endothelial cells of the embryonic forebrain. As schizophrenia topped the list of disease categories, we identified some of the top common genes that were enriched in this category in periventricular endothelial cells after comparisons with both pial and control endothelial cells (Supplementary Data 1). In diseases like schizophrenia, epilepsy and autism, abnormalities have been widely reported in GABA neurons^{3, 4, 33}, with increasing evidence that this may be in part due to incorrect differentiation and misguided migration of GABA neurons during brain development^{34, 35}. Interestingly, in our screen we found many genes commonly known to be expressed and/or traditionally believed to be confined to GABA neurons/interneurons and their precursors were expressed/up-regulated in periventricular endothelial cells (Supplementary Table S1) and some in pial endothelial cells (Supplementary Table S2). Some of the top genes were subdivided into categories like transcription factors, cell-surface molecules essential for migration and genes related to ionic regulation that are involved in GABA signalling (Supplementary Tables S1 & S2). For validation of differentially expressed genes, quantitative real-time PCR was performed on eight randomly picked genes, *Gabrb3*, *Gabra1*, *Cxcr4*, *Cdk5r1*, *Foxg1* and *Sez6l2c* (Fig. 5c). Each of these genes were several fold upregulated in periventricular endothelial cells (Fig. 5c).

Endothelial GABA_A receptors modulate GABA neuron migration

GABA_A receptors are traditionally believed to be confined to GABA neurons, but our microarray and real-time PCR data detected high expression of these receptors in periventricular endothelial cells (Supplementary Table S1, Fig. 5c) signifying that telencephalic angiogenesis has its own intrinsic GABA signaling mechanism. GABA and its receptors-mediated signaling have been suggested to modulate progenitor cell proliferation, neuronal migration and circuit formation in the cortex^{36–38}. Defects in GABA_A receptor regulation has been suggested as a mechanism contributing to schizophrenia, epilepsy and autism^{39–41}. Although there are reports of presence of GABA_A receptors on blood vessel membranes, atria, left ventricle, descending aorta and in the endothelium lining of the vasculature of brain^{42, 43}, GAD immunoreactivities in endothelial cells of cerebral arteries⁴⁴, GAD65 expression by *in situ* hybridization in cardiac arteries and major blood vessels of E12.5 embryo⁴⁵, its functional significance remains unknown. Therefore, we selected one of the validated genes in periventricular endothelial cells, GABA_A receptor, *Gabrb3*, associated with psychiatric and neurodevelopmental disorders^{2, 46–51} to test its autonomous role in periventricular endothelial cells. Co-labeling with isolectin B4 and GABRB3 antibodies showed robust expression of GABRB3 in periventricular endothelial cells (Fig. 6a, b). GFP+ve endothelial cells from Tie2-GFP mouse brains confirmed GABRB3 expression in periventricular endothelial cells (Fig. 6c). When GABRB3 expression was

down-regulated in periventricular endothelial cells by siRNA technique (Fig. 6d), there was a marked decrease in endothelial cell proliferation (Fig. 6e) confirming its role in periventricular angiogenesis. Subsequently, GE explants showed a lack of chemoattraction towards *Gabrb3* siRNA-transfected endothelial cells when compared to the respective control (Fig. 6f–i). In addition, loss of function of *Gabrb3* in periventricular endothelial cells significantly decreased cell migration from GE explants (Fig. 6j, k) alone. Since sps cells do not migrate on periventricular endothelial cells (Fig. 3f, i), the migratory response of sps cells on control and siRNA transfected ecs remained comparable (Fig. 6k) Thus, *Gabrb3* siRNA-transfected periventricular endothelial cells were unable to provide chemoattractive and guidance cues that are needed for GABA neuron migration. Interestingly, loss of function of GABRB3 down-regulated GABA expression in periventricular endothelial cells when compared to the respective control (Fig. 6l–o). GABA is known to act as a chemoattractant, providing directional cues to migrating neurons and enhancing chemotaxis or chemokinesis in the developing telencephalon^{37, 38, 52–54}. Hence we investigated for detection of secreted GABA by ELISA from control and *Gabrb3* siRNA-transfected periventricular endothelial cells. While control siRNA-transfected periventricular endothelial cells secreted GABA, in sharp contrast, GABA secretion was abolished from *Gabrb3* siRNA-transfected periventricular endothelial cells (Fig. 6p).

Since *Gabra2* was the only GABA_A receptor identified from our microarray screen in pial endothelial cells (Supplementary Table S2), we tested if it might have a role in pial angiogenesis. Expression of GABRA2 in pial endothelial cells was confirmed by co-labeling with isolectin B4 and GABRA2 antibodies (Fig. 7a, b). Pial endothelial cells from Tie2-GFP mouse brains revealed GABRA2 expression (Fig. 7c). Downregulation of GABRA2 expression in pial endothelial cells (Fig. 7d) resulted in a significant decrease in endothelial cell proliferation (Fig. 7e) confirming its role in pial angiogenesis. A decrease in chemoattractive response of sps explants towards *Gabra2* siRNA-transfected pial endothelial cells was observed (Fig. 7f–i). Cell migration from sps explants was significantly decreased on substrates of *Gabra2* siRNA-transfected pial endothelial cells when compared to the respective control (Fig. 7j, k). Cells from GE explants showed reduced migration on pial endothelial cell substrates whether they were transfected with control siRNA (similar to our observations in Fig. 3c, e) or *Gabra2* siRNA (Fig. 7k). Thus, *Gabra2* siRNA-transfected pial endothelial cells were unable to provide the necessary cues required by superficial GABA neurons. Furthermore, down-regulation of GABRA2 significantly decreased GABA expression in pial endothelial cells when compared to the respective control (Fig. 7l–o). Interestingly control pial endothelial cells secreted GABA (Fig. 7p) at approximately two fold higher levels than control periventricular endothelial cells (Fig. 6p). *Gabra2* siRNA-transfected pial endothelial cells failed to secrete GABA (Fig. 7p) similar to *Gabrb3* siRNA-transfected periventricular endothelial cells (Fig. 6p). Our results not only depict a new vascular source of GABA in the early embryonic telencephalon but also suggest that deep GABA neurons respond to low levels of GABA secreted by periventricular endothelial cells and superficial GABA neurons respond to higher levels of GABA secreted by pial endothelial cells (Fig. 7q, r). Our data signifies a novel mechanism of endothelial cell-mediated segregation and migration of GABA neurons in the embryonic telencephalon.

Discussion

The results of our studies are notable for several reasons. First, they reveal that pre-formed embryonic vascular networks are strategically positioned to fulfill the formidable task of providing support and guidance cues to GABA neurons on their lengthy tangential journey in the telencephalon. For the treatment of neurodegenerative diseases a promising approach has been the transplantation of neuronal precursors into the adult brain. But, transplanted primary neuronal precursors have often been reported to remain at transplantation sites and are unable to migrate and integrate into regions that require new neurons^{55, 56}. This is usually explained by the absence of substrates to aid neuronal migration like radial glial guides. The versatile periventricular endothelial cells of the embryonic telencephalon may offer a solution for stalled neuronal precursors at transplantation sites. Second, they highlight the importance of endothelial cell diversity and function in the embryonic telencephalon and pave way to many important questions regarding specifically expressed genes in individual populations of endothelial cells based on their position in the CNS. Third, our results potentially implicate a new cell type - periventricular endothelial cells as being contributory to a wide swath of neurological and psychiatric diseases. For example, the observation that many of the genes linked to schizophrenia are expressed in periventricular endothelial cells will initiate future studies of this disease from a new perspective. In schizophrenia, multiple pathways in different cell types likely co-exist in patients synergistically inducing the highly complex form of this disease; and it is crucial to understand the autonomous program of these endothelial cells with respect to this disease. And finally, genes believed to independently regulate GABA neurogenesis and migration were expressed predominantly in periventricular endothelial cells signifying that the periventricular angiogenesis gradient and GABA neuron developmental gradients are related to one another at mechanistic levels. The presence of GABA_A receptors on periventricular and pial endothelial cells and secretion of different levels of GABA by these populations of endothelial cells that has critical functions in attracting and promoting neuronal migration reveals a novel mechanism of GABA and its receptors' signaling in the CNS (Fig. 7q, r). A role for GABA_A receptor - GABA signaling in angiogenesis with consequences for GABA neuron migration opens new doors to pursue many questions in brain development and diseases that result from abnormal brain development like schizophrenia, epilepsy and autism.

As we appreciate the new roles of periventricular angiogenesis, we begin also to encounter an important problem from another viewpoint. The problem is very significant indeed given that we have focused on neurological and psychiatric illnesses from a neuronal perspective extensively and it emphasizes the critical need to not underestimate the vasculature so intimately associated with neurons. The pioneering periventricular endothelial cells of the telencephalon, that develop in advance of and free of neuronal development hold a valuable key for the establishment of the later forming neuronal networks and point to a novel paradigm of endothelial cell – neuron interactions in the embryonic forebrain.

Methods

Animals

Timed pregnant CD1 mice (E13) were purchased from Charles River laboratories, MA. Colonies of GAD65-GFP and Tie2-GFP mice were maintained in our institutional animal facility. The day of plug discovery was designated embryonic day 0 (E0). Animal experiments were in full compliance with the NIH Guide for Care and Use of Laboratory Animals and were approved by the McLean Institutional Animal Care Committee.

Slice preparation and immunohistochemistry

Brains from E13 GAD65-GFP embryos were collected and fixed in 4% paraformaldehyde at 4°C. Vibratome slices (50 µm) were prepared and incubated in anti-biotinylated isolectinB4 (1:40, Sigma) with 1% TritonX-100 at 4°C overnight. After six washes in PBS, slices were incubated with secondary antibody (Alexa 594 streptavidin conjugate) for 6 hours at 4°C. Flat mounted samples were analyzed by a Zeiss LSM 5 Pascal laser confocal microscope. Images of the entire telencephalon were collected along the Z-axis. The distance of GABA neurons to blood vessels was calculated from high-power Z-stack confocal images using ImageJ software.

Embryonic brains from E13 CD1 mice were immersed in zinc fixative (BD Pharmingen) for 24 hours and processed for paraffin histology. Double labeling immunohistochemistry was performed on 20 µm thick paraffin embedded sections with anti-biotinylated isolectinB4 (1:40, Sigma) and rabbit polyclonal anti-GAD65/GAD67 (Millipore, 1:400) antibodies. Secondary antibodies used were Anti-rabbit Alexa fluor 594 conjugate and Streptavidin Alexa fluor 488 conjugate (Molecular Probes).

Isolation and primary culture of endothelial cells

E13 CD1 embryonic brains were dissected under a stereo-microscope and the telencephalon was removed. Pial membranes were peeled out and pooled (pial endothelial cells). The remaining telencephalon without pial membranes was pooled as well (periventricular endothelial cells). Mesencephalon and metencephalon were combined to prepare control endothelial cells. Purity of endothelial cell cultures was established with endothelial cell markers and determined to be a hundred percent⁵. Isolation and culture of endothelial cells of the three sets were performed according to published methodology⁵.

Chemoattraction and slice culture experiments

In preparation for the chemoattraction assays, square culture inserts (ibidi GmbH) were placed in the center of 35mm collagen coated culture dishes, to create a barrier (width - 0.9 cm). Cultures of periventricular and pial endothelial cells were trypsinized and plated on either side of the barrier (experimental strategy outlined in text and Fig. 2b). To prepare explants, GAD65-GFP+ve brains were cut at a thickness of 250 µm on a vibratome coronally. The ganglionic eminence (GE) region as well as sub-pial surface of ventral telencephalon (sps) were micro-dissected and further trimmed into blocks of equal size respectively (All sps explant blocks were longer since they were isolated closely along the length of the subpial surface whereas GE explant blocks were wider). Individual explants

were plated in the barrier-free area of the plate with pial and periventricular endothelial cells on either side. The co-culture was maintained for 24 hrs in FCS-DMEM (Invitrogen). At the end of the experiment, Tritc-conjugated isolectin B4 antibody (1:50, Sigma) was used to quickly label and visualize endothelial cells during subsequent imaging. The chemoattractive response of GFP+ve cells from the explant towards endothelial cells in each experiment were imaged and saved as JPEG files.

In a parallel set of experiments the same set of explants were plated on thin sheets of Geltrex™ basement membrane matrix (Invitrogen) that had been previously seeded with pial, periventricular or control endothelial cells. Following 12 hrs *in vitro* the cultures were fixed in 4% paraformaldehyde and migration of GFP+ cells were analyzed. Images were taken and saved as TIFF files. The number and distance of migrating GFP+ve cells relative to the edge of the explant in all quadrants was calculated using ImageJ software and plotted.

For disruption of pial and periventricular vascular networks, whole telencephalon explants prepared from E12 GAD65-GFP brains were transferred to polycarbonate membrane filters (8 μm pore size; Gibco-Life Technologies) in sterile 6 well plates, incubated with Neurobasal™ medium (1x, Gibco) and cultured for 36 hours. For the bead experiments, heparin beads (Sigma) were washed thrice in PBS and soaked in angiogenesis inhibitor - TNP-470 (Sigma, 10μg) for 1–2 hr at room temperature. Prior to implantation into the ventricular zone of the dorsal telencephalon, beads were washed in neurobasal medium. Control beads were treated identically with 0.1% BSA in PBS. To inhibit pial angiogenesis, 6-hydroxydopamine hydrochloride (6-OHDA, Sigma, 10μg/ml) was added to the culture medium. At the end of the experiment, explants were fixed in 4% paraformaldehyde, cryoprotected in sucrose gradient, embedded into frozen blocks and sectioned at 40 μm on a cryostat. Blood vessels were labeled with biotinylated isolectinB4 (1:40, Sigma) followed by secondary detection with Streptavidin Alexa fluor 594 conjugate. Dorsal telencephalon was imaged and images were saved as TIFF files. The density of GFP+ve cells in the selected areas was calculated from high magnification individual images using ImageJ software. Statistical significance of differences between groups in all sets of experiments was analyzed by two-tailed Student's t-test (Prism; GraphPad software).

Fluorescence-activated cell sorting and RNA preparation

Three sets of samples from E13 Tie2-GFP brains (in which endothelial cells express GFP specifically⁵): 1) Pial membranes from the telencephalon, 2) telencephalon without pia and 3) combined mesencephalon and metencephalon regions were individually minced into 1–2 mm fragments with a scalpel, rinsed in PBS and incubated at 37°C for 30 min in pre-warmed PBS with trypsin (0.25%), DNase I (1 mg/ml) and EDTA (0.5mM). Cells were dissociated, spun down, re-suspended in warm 10% FCS-DMEM and filtered through a sterile 100μm nylon mesh. Cells were re-suspended in 1 ml RBC lysing buffer (Sigma), overlaid onto DMEM and centrifuged. Cells were washed with ice-cold FACS buffer (2% FCS and 0.1% NaN₃ in PBS) and incubated with Fcγ blocker (BD Biosciences Pharmingen, 1μg/ml) for 30 min. Cells were washed in ice-cold FACS buffer and stained with anti-CD31 APC conjugated antibody (ebioscience) for 1 hr. Cells were washed in ice-cold FACS buffer and GFP⁺/CD-31⁺ endothelial cells were purified by fluorescence-activated cell sorting

using a BD FACSAria-II flow cytometer (BD Biosciences, San Jose, CA). The gating parameters are slightly different because the experiments were performed at different days and the auto-fluorescence (background fluorescence) of the samples varied and the settings of the flow cytometer were different based on the background fluorescence. Thus, we gated in order to sort specifically GFP⁺ population that were homogeneously expressing CD31 at a similar level. GFP fluorescence in purified endothelial cells was verified before RNA isolation. RNA was extracted from purified endothelial cells using the PicoPure™ RNA Isolation kit (Arcturus). RNA was shipped to Precision Biomarker Resources Inc, Evanston, IL where RNA quality was determined and microarray hybridization was performed.

Gene expression profile analysis

Affymetrix's Probe Logarithmic Intensity Error (PLIER) signal of "15" was used as the evidence of gene expression. The ratio of "Periventricular"/"Pial" > 2.0 fold was arbitrarily considered as "Periventricular"-favored gene activity and "Pial"/"Periventricular" > 2.0 fold as "Pial"-favored gene activity. The ratio of "Periventricular"/"Control" > 2.0 fold was arbitrarily considered as "Periventricular"-favored gene activity and "Control"/"Periventricular" > 2.0 fold as "Control"-favored gene activity. The lists of favored genes were subjected to a series of Enrichment GeneGo Ontology (Pathway Maps⁵⁷, Biomarker-based Disease Category and Process Networks) as well as Go Processes and Go Molecular Functions analyses in MetaCore or literature survey for cell type-specific genes. The $-\text{LOG}_{10}$ (*P*-value for significance) was used as enrichment score. "Periventricular" and "Pial" were analyzed side-by-side and "Periventricular" and "control" were analyzed side by side for the sake of comparison unless indicated elsewhere.

Real-time PCR

RT was performed by using transcriptor first-strand cDNA synthesis kit (Roche Diagnostic). PCR reactions were run on an ABI Prism 7500 (Applied Biosystems) sequence detection system platform. Taqman primers with 6-carboxyfluorescein probe for *Gabrb3*, *Gabra1*, *Cxcr4*, *Cdk5r1*, *Foxg1* and *Sez6l2c* were obtained from Applied Biosystems. The house keeping gene $\beta 2$ microglobulin was used as a control. The relative gene expression among different samples and subsequent fold increase in periventricular versus pial endothelial cells was determined according to published methodology⁵⁸.

Endothelial cell stainings and cell migration assays

Periventricular and pial endothelial cells were prepared from both CD1 and Tie2-GFP embryos. Periventricular endothelial cells were labeled with anti-GABRB3 (Sigma, 1:200) and pial endothelial cells were labeled with anti-GABRA2 (Synaptic Systems, 1:400). Anti-biotinylated isolectinB4 (1:40, Sigma) was used for co-labeling and DAPI (Invitrogen) was used to label nuclei. Images were taken on an FSX100 microscope (Olympus). For siRNA transfections, pre-designed siRNA constructs for *Gabrb3*, *Gabra2* and a control non-targeting siRNA (Dharmacon) were used. Transfection of endothelial cells maintained at 80% confluency in six well plates, cell harvest, lysis, blots and cell proliferation assays were performed according to published methodology⁵. Chemoattraction and migration assays were performed with transfected endothelial cells using similar methods described earlier.

After 96 hours of transfection, endothelial cells were processed for GABA immunohistochemistry (anti-GABA, Sigma, 1:400). Supernatants were also collected after 96 hours of transfection and stored at -80°C for ELISA. GABA concentrations were quantitatively determined by competitive ELISA according to manufacturers' protocol (GABA Research ELISA kits, Labor Diagnostica Nord, Germany), and absorbance was measured using a multiplate microplate fluorescence reader (Molecular Devices, CA) at 450 nm.

Supplementary Material

Refer to Web version on PubMed Central for supplementary material.

Acknowledgements

This work was supported by a National Alliance for Research on Schizophrenia and Depression (NARSAD) Young Investigator Award and National Institutes of Health grants R21NS064386 and R01NS073635 to AV.

References

1. Treiman DM. GABAergic mechanisms in epilepsy. *Epilepsia*. 2001; 42(Suppl. 3):8–12. [PubMed: 11520315]
2. Marin O. Interneuron dysfunction in psychiatric disorders. *Nat Rev Neurosci*. 2012; 13:107–120. [PubMed: 22251963]
3. Levitt P, Eagleson KL, Powell EM. Regulation of neocortical interneuron development and the implications for neurodevelopmental disorders. *Trends Neurosci*. 2004; 27:400–406. [PubMed: 15219739]
4. Lewis DA, Hashimoto T, Volk DW. Cortical inhibitory neurons and schizophrenia. *Nat Rev Neurosci*. 2005; 6:312–324. [PubMed: 15803162]
5. Vasudevan A, Long JE, Crandall JE, Rubenstein JL, Bhide PG. Compartment-specific transcription factors orchestrate angiogenesis gradients in the embryonic brain. *Nat Neurosci*. 2008; 11:429–439. [PubMed: 18344991]
6. Vasudevan A, Bhide PG. Angiogenesis in the embryonic CNS: a new twist on an old tale. *Cell Adh Migr*. 2008; 2:167–169. [PubMed: 19262109]
7. Hogan KA, Ambler CA, Chapman DL, Bautch VL. The neural tube patterns vessels developmentally using the VEGF signaling pathway. *Development*. 2004; 131:1503–1513. [PubMed: 14998923]
8. Lopez-Bendito G, et al. Preferential origin and layer destination of GAD65-GFP cortical interneurons. *Cereb Cortex*. 2004; 14:1122–1133. [PubMed: 15115742]
9. Marin O, Rubenstein JL. A long, remarkable journey: tangential migration in the telencephalon. *Nat Rev Neurosci*. 2001; 2:780–790. [PubMed: 11715055]
10. Corbin JG, Nery S, Fishell G. Telencephalic cells take a tangent: non-radial migration in the mammalian forebrain. *Nat Neurosci*. 2001; 4(Suppl):1177–1182. [PubMed: 11687827]
11. Parnavelas JG. The origin and migration of cortical neurones: new vistas. *Trends Neurosci*. 2000; 23:126–131. [PubMed: 10675917]
12. Hatten ME. New directions in neuronal migration. *Science*. 2002; 297:1660–1663. [PubMed: 12215636]
13. Rakic P. Specification of cerebral cortical areas. *Science*. 1988; 241:170–176. [PubMed: 3291116]
14. Lois C, Garcia-Verdugo JM, Alvarez-Buylla A. Chain migration of neuronal precursors. *Science*. 1996; 271:978–981. [PubMed: 8584933]
15. Denaxa M, Chan CH, Schachner M, Parnavelas JG, Karagogeos D. The adhesion molecule TAG-1 mediates the migration of cortical interneurons from the ganglionic eminence along the corticofugal fiber system. *Development*. 2001; 128:4635–4644. [PubMed: 11714688]

16. O'Rourke NA, Sullivan DP, Kaznowski CE, Jacobs AA, McConnell SK. Tangential migration of neurons in the developing cerebral cortex. *Development*. 1995; 121:2165–2176. [PubMed: 7635060]
17. Tanaka D, Nakaya Y, Yanagawa Y, Obata K, Murakami F. Multimodal tangential migration of neocortical GABAergic neurons independent of GPI-anchored proteins. *Development*. 2003; 130:5803–5813. [PubMed: 14534141]
18. Marin O, et al. Directional guidance of interneuron migration to the cerebral cortex relies on subcortical Slit1/2-independent repulsion and cortical attraction. *Development*. 2003; 130:1889–1901. [PubMed: 12642493]
19. Marin O, Rubenstein JL. Cell migration in the forebrain. *Annu Rev Neurosci*. 2003; 26:441–483. [PubMed: 12626695]
20. Wichterle H, Alvarez-Dolado M, Erskine L, Alvarez-Buylla A. Permissive corridor and diffusible gradients direct medial ganglionic eminence cell migration to the neocortex. *Proc Natl Acad Sci U S A*. 2003; 100:727–732. [PubMed: 12515855]
21. Yuan W, et al. The mouse SLIT family: secreted ligands for ROBO expressed in patterns that suggest a role in morphogenesis and axon guidance. *Dev Biol*. 1999; 212:290–306. [PubMed: 10433822]
22. Skaliora I, Singer W, Betz H, Puschel AW. Differential patterns of semaphorin expression in the developing rat brain. *Eur J Neurosci*. 1998; 10:1215–1229. [PubMed: 9749776]
23. Marin O, Yaron A, Bagri A, Tessier-Lavigne M, Rubenstein JL. Sorting of striatal and cortical interneurons regulated by semaphorin-neuropilin interactions. *Science*. 2001; 293:872–875. [PubMed: 11486090]
24. Flames N, et al. Short- and long-range attraction of cortical GABAergic interneurons by neuregulin-1. *Neuron*. 2004; 44:251–261. [PubMed: 15473965]
25. Powell EM, Mars WM, Levitt P. Hepatocyte growth factor/scatter factor is a motogen for interneurons migrating from the ventral to dorsal telencephalon. *Neuron*. 2001; 30:79–89. [PubMed: 11343646]
26. Zhu Y, Li H, Zhou L, Wu JY, Rao Y. Cellular and molecular guidance of GABAergic neuronal migration from an extracortical origin to the neocortex. *Neuron*. 1999; 23:473–485. [PubMed: 10433260]
27. Stumm RK, et al. CXCR4 regulates interneuron migration in the developing neocortex. *The Journal of neuroscience : the official journal of the Society for Neuroscience*. 2003; 23:5123–5130. [PubMed: 12832536]
28. Pozas E, Ibanez CF. GDNF and GFRalpha1 promote differentiation and tangential migration of cortical GABAergic neurons. *Neuron*. 2005; 45:701–713. [PubMed: 15748846]
29. Polleux F, Whitford KL, Dijkhuizen PA, Vitalis T, Ghosh A. Control of cortical interneuron migration by neurotrophins and PI3-kinase signaling. *Development*. 2002; 129:3147–3160. [PubMed: 12070090]
30. Tiveron MC, et al. Molecular interaction between projection neuron precursors and invading interneurons via stromal-derived factor 1 (CXCL12)/CXCR4 signaling in the cortical subventricular zone/intermediate zone. *The Journal of neuroscience : the official journal of the Society for Neuroscience*. 2006; 26:13273–13278. [PubMed: 17182777]
31. Ingber D, et al. Synthetic analogues of fumagillin that inhibit angiogenesis and suppress tumour growth. *Nature*. 1990; 348:555–557. [PubMed: 1701033]
32. Castronovo V, Belotti D. TNP-470 (AGM-1470): mechanisms of action and early clinical development. *Eur J Cancer*. 1996; 32A:2520–2527. [PubMed: 9059342]
33. DeFelipe J. Chandelier cells and epilepsy. *Brain*. 1999; 122(Pt 10):1807–1822. [PubMed: 10506085]
34. Lewis DA, Levitt P. Schizophrenia as a disorder of neurodevelopment. *Annu Rev Neurosci*. 2002; 25:409–432. [PubMed: 12052915]
35. Benes FM, Berretta S. GABAergic interneurons: implications for understanding schizophrenia and bipolar disorder. *Neuropsychopharmacology*. 2001; 25:1–27. [PubMed: 11377916]
36. Wang DD, Kriegstein AR. Defining the role of GABA in cortical development. *J Physiol*. 2009; 587:1873–1879. [PubMed: 19153158]

37. Behar TN, Schaffner AE, Scott CA, Greene CL, Barker JL. GABA receptor antagonists modulate postmitotic cell migration in slice cultures of embryonic rat cortex. *Cereb Cortex*. 2000; 10:899–909. [PubMed: 10982750]
38. Heck N, et al. GABA-A receptors regulate neocortical neuronal migration in vitro and in vivo. *Cereb Cortex*. 2007; 17:138–148. [PubMed: 16452638]
39. Petryshen TL, et al. Genetic investigation of chromosome 5q GABAA receptor subunit genes in schizophrenia. *Mol Psychiatry*. 2005; 10:1074–1088. 1057. [PubMed: 16172613]
40. Kang JQ, Macdonald RL. Making sense of nonsense GABA(A) receptor mutations associated with genetic epilepsies. *Trends Mol Med*. 2009; 15:430–438. [PubMed: 19717338]
41. Fatemi SH, Reutiman TJ, Folsom TD, Thuras PD. GABA(A) receptor downregulation in brains of subjects with autism. *J Autism Dev Disord*. 2009; 39:223–230. [PubMed: 18821008]
42. Tyagi N, et al. Differential expression of gamma-aminobutyric acid receptor A (GABA(A)) and effects of homocysteine. *Clin Chem Lab Med*. 2007; 45:1777–1784. [PubMed: 17990949]
43. Ong J, Kerr DI. GABA-receptors in peripheral tissues. *Life Sci*. 1990; 46:1489–1501. [PubMed: 2162457]
44. Imai H, Okuno T, Wu JY, Lee TJ. GABAergic innervation in cerebral blood vessels: an immunohistochemical demonstration of L-glutamic acid decarboxylase and GABA transaminase. *J Cereb Blood Flow Metab*. 1991; 11:129–134. [PubMed: 1983997]
45. Katarova Z, Sekerkova G, Prodan S, Mugnaini E, Szabo G. Domain-restricted expression of two glutamic acid decarboxylase genes in midgestation mouse embryos. *J Comp Neurol*. 2000; 424:607–627. [PubMed: 10931484]
46. Bergen SE, Fanous AH, Walsh D, O'Neill FA, Kendler KS. Polymorphisms in SLC6A4, PAH, GABRB3, and MAOB and modification of psychotic disorder features. *Schizophr Res*. 2009; 109:94–97. [PubMed: 19268543]
47. Sun J, Jayathilake K, Zhao Z, Meltzer HY. Investigating association of four gene regions (GABRB3, MAOB, PAH, and SLC6A4) with five symptoms in schizophrenia. *Psychiatry Res*. 2012
48. DeLorey TM, et al. Mice lacking the beta3 subunit of the GABAA receptor have the epilepsy phenotype and many of the behavioral characteristics of Angelman syndrome. *J Neurosci*. 1998; 18:8505–8514. [PubMed: 9763493]
49. DeLorey TM, Olsen RW. GABA and epileptogenesis: comparing gabrb3 gene-deficient mice with Angelman syndrome in man. *Epilepsy Res*. 1999; 36:123–132. [PubMed: 10515160]
50. DeLorey TM. GABRB3 gene deficient mice: a potential model of autism spectrum disorder. *Int Rev Neurobiol*. 2005; 71:359–382. [PubMed: 16512358]
51. DeLorey TM, Sahbaie P, Hashemi E, Homanics GE, Clark JD. Gabrb3 gene deficient mice exhibit impaired social and exploratory behaviors, deficits in non-selective attention and hypoplasia of cerebellar vermal lobules: a potential model of autism spectrum disorder. *Behav Brain Res*. 2008; 187:207–220. [PubMed: 17983671]
52. Behar TN, et al. GABA stimulates chemotaxis and chemokinesis of embryonic cortical neurons via calcium-dependent mechanisms. *The Journal of neuroscience : the official journal of the Society for Neuroscience*. 1996; 16:1808–1818. [PubMed: 8774448]
53. Behar TN, Schaffner AE, Scott CA, O'Connell C, Barker JL. Differential response of cortical plate and ventricular zone cells to GABA as a migration stimulus. *The Journal of neuroscience : the official journal of the Society for Neuroscience*. 1998; 18:6378–6387. [PubMed: 9698329]
54. Varju P, Katarova Z, Madarasz E, Szabo G. GABA signalling during development: new data and old questions. *Cell Tissue Res*. 2001; 305:239–246. [PubMed: 11545261]
55. Graybiel AM, Liu FC, Dunnett SB. Intrastratial grafts derived from fetal striatal primordia. I. Phenotypy and modular organization. *The Journal of neuroscience : the official journal of the Society for Neuroscience*. 1989; 9:3250–3271. [PubMed: 2477513]
56. Wichterle H, Garcia-Verdugo JM, Herrera DG, Alvarez-Buylla A. Young neurons from medial ganglionic eminence disperse in adult and embryonic brain. *Nat Neurosci*. 1999; 2:461–466. [PubMed: 10321251]
57. Ekins S, Nikolsky Y, Bugrim A, Kirillov E, Nikolskaya T. Pathway mapping tools for analysis of high content data. *Methods Mol Biol*. 2007; 356:319–350. [PubMed: 16988414]

58. Pfaffl MW. A new mathematical model for relative quantification in real-time RT-PCR. *Nucleic Acids Res.* 2001; 29:e45. [PubMed: 11328886]

Author Manuscript

Author Manuscript

Author Manuscript

Author Manuscript

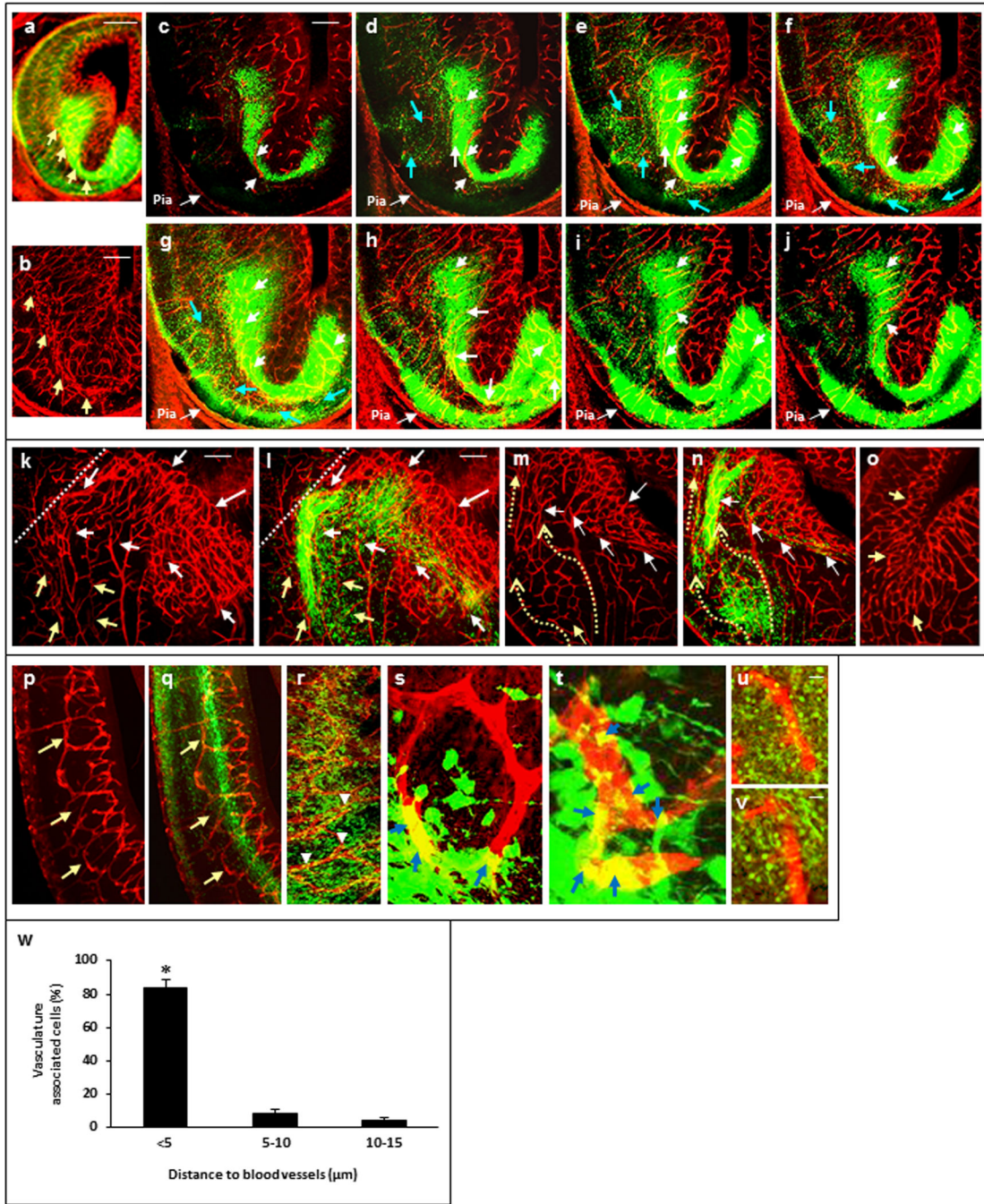


Figure 1. GABA neurons are closely associated with vascular networks in the early embryonic telencephalon

(a) Surface view of an E13 GAD65-GFP telencephalon (vibratome section, 50 μm , coronal) labeled with isolectin B4. (b) Confocal image depicting vascular profile in the ventral telencephalon. Yellow arrows (a, b) point out tangential direction of periventricular vessels that support deep GABA neuron stream towards PSB. (c–j) The ventral telencephalon of the section in ‘a’ was studied by confocal microscopy. White arrows point to deep GABA neuron stream enwrapped in the periventricular network. Blue arrows point to GABA neurons segregating out to form the second stream close to the pial network. (k–n)

Periventricular vascular profile close to PSB and in the GE (k) and the GABA neuron stream (l) associated with it at rostral (k, l) and caudal (m, n) levels. White dotted line marks PSB. Yellow arrows point out periventricular vascular profile leading towards PSB. White arrows points to the continuous plexus of periventricular vessels of the GE that connects to vessels near the PSB. Observe the vascular profile between the yellow dotted arrows (m, n) that channels GABA neurons towards PSB. (o) The lattice arrangement of periventricular vessels at the PSB continues into the SVZ region of the dorsal telencephalon (yellow arrows). (p–q) The periventricular vascular profile in the dorsal telencephalon (yellow arrows, p) and the deep stream of GABA neurons in close contact with the periventricular network (q). (r) The periventricular network is studded with GABA neurons (white arrowheads). (s–t) A magnified periventricular lattice (s) and vessel (t) showing intimate direct contact with GABA neurons (co-label in yellow, blue arrows). (u–v) Paraffin sections (20 μm) from E13 CD1 telencephalon were co-labeled with isolectin B4 (red) and GAD65/67 (green) markers. A 40x magnification from ventral (u) and dorsal (v) telencephalon shows processes of GABA neurons wrapped around periventricular vessels. (w) Quantification of vasculature associated GABA neurons in the telencephalon using Image-J software. Data represents mean \pm SD (n=25, *P < 0.0001, Student's t-test, group '< 5 μm ' compared to group '< 5–10 μm '). Scale bars: a, 200 μm ; b, 100 μm (applies b–t); u, 50 μm (applies to v). GE: ganglionic eminence, PSB: pallial-subpallial boundary, SVZ: subventricular zone.

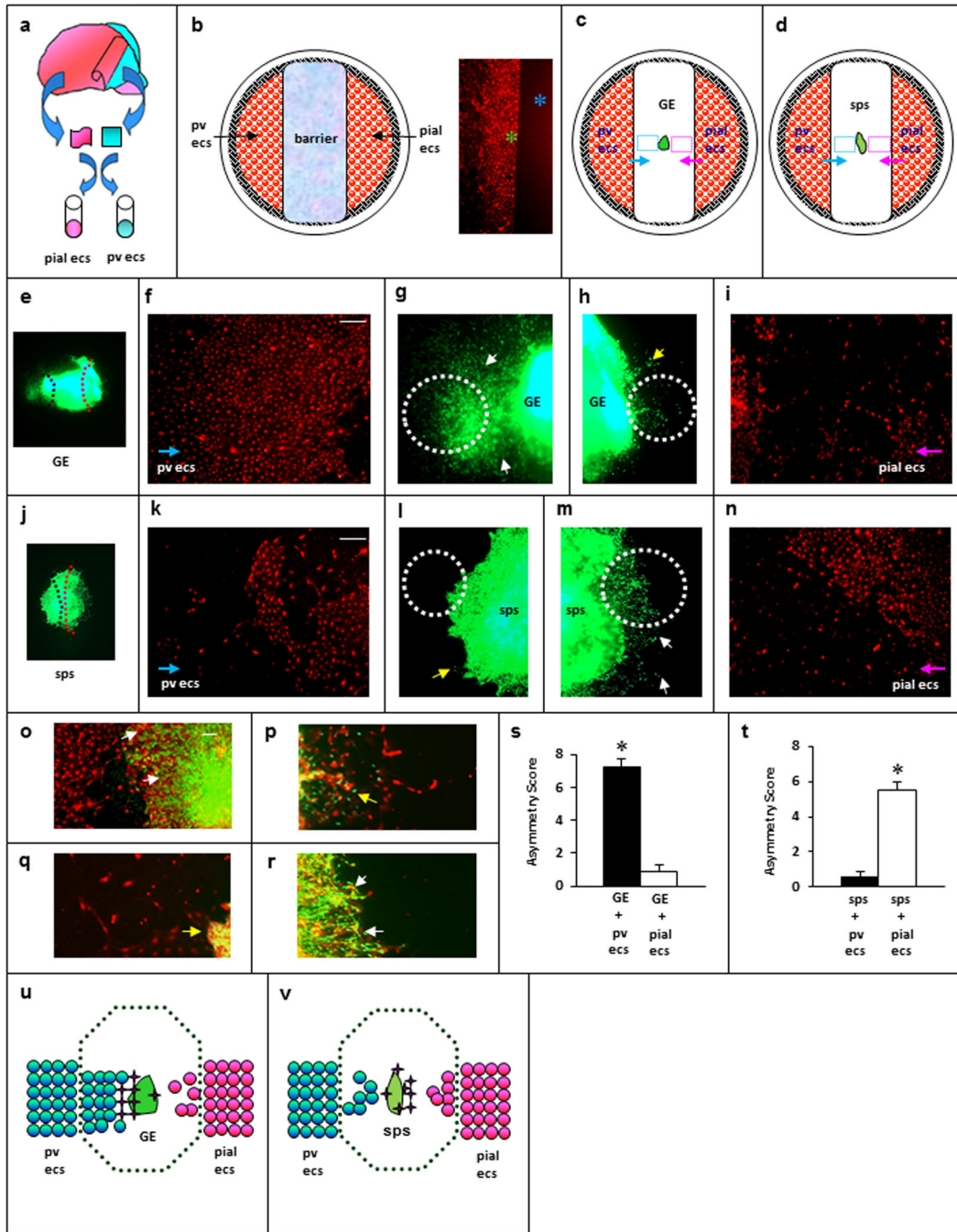


Figure 2. Selective chemoattractive responses of GABA neurons towards pial and periventricular endothelial cells

(a) Experiment schematic of isolation of pial and periventricular (pv) endothelial cells (ecs).
 (b) Diagram depicting preparation for chemoattractivity experiment. Ecs at barrier edge (green star) form a straight line with no escape into barrier occupied area (blue star) ensuring barrier reliability. (c–d) Schema of GE (dark green, c) and sps (light green, d) explants co-cultured with pv and pial ecs. Blue and pink dotted rectangles (c, d) depict areas of pv and pial ecs migration towards the explant in images f, i, k and n. Blue arrows (c, d) indicate direction of pv ecs migration (f, k) and pink arrows (c, d) indicate direction of pial ecs

migration (i, n) towards the explant. (e–r) Robust chemoattractive activity in GE explant towards pv ecs only and significant chemoattractive activity in sps explant towards pial ecs only. Left half (black dots) of the explants (e and j) were magnified in g and l and right half (red dots) of the explants (e, j) were magnified in h and m. White dotted circles in g, h, l and m are magnified in o–r and depict co-labeling of neurons and ecs. Co-labeled images of the chemoattractive response of GE (o, p) and sps (q, r) derived GABA neurons towards pv (o, q) and pial (p, r) ecs. White arrows point to significant chemoattractive responses from explants (g, m, o, r) and yellow arrows point out little response from explants (h, l, p, q). (s–t) Quantification of chemoattraction of GE (s) and sps (t) explant towards pv and pial ecs; Data represents mean \pm SD (n=20, *P < 0.0001, Student's t-test); scoring scheme applied from reference²⁴. (u–v) Summary diagram from c–t (n=20). Green stars depict chemoattractive activity from GE and sps explants, blue circles represent pv ecs and pink circles represent pial ecs. Robust migration of pv ecs towards GE explant was observed when compared to pial ecs. Robust chemoattractivity of GE explants to pv ecs only (u) and sps explants to pial ecs only (v). Scale bars: f, 100 μ m (applies also to g–i, k–m); o, 50 μ m (applies also to p–r).

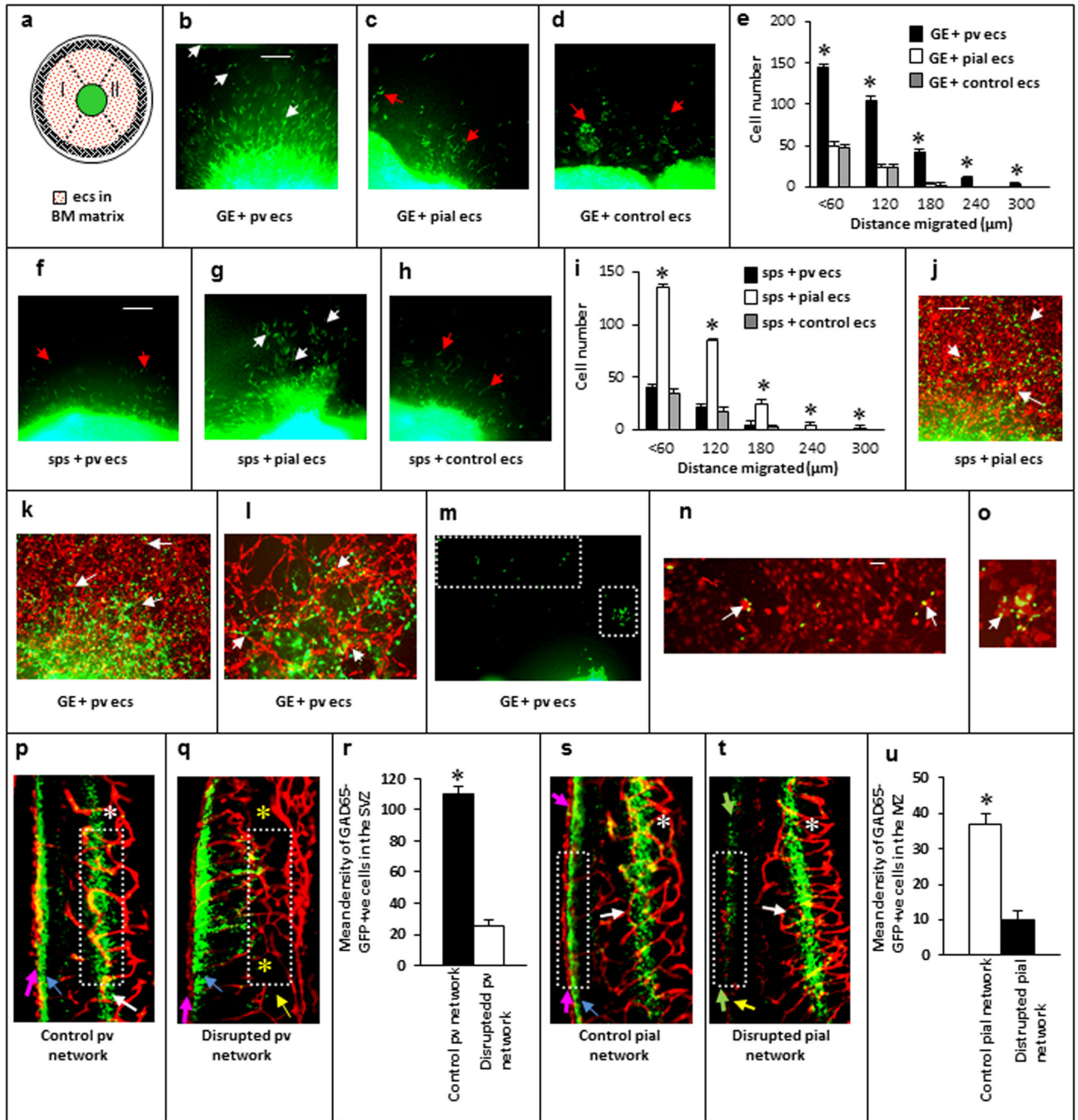


Figure 3. Endothelial cells provide cues for selective sorting and migration of individual streams of GABA neurons

(a) Experiment schematic: Either pv, pial or control ecs were seeded in BM matrix and cell migration from GE or sps explants was analyzed in sectors I and II. (b–i) Robust migration of GE derived cells in response to pv ecs compared to pial and control ecs (b–e) and robust migration of sps derived cells in response to pial ecs compared to pv and control ecs (f–i). White arrows point to robust migration and red arrows point to little migration. (e & i) Quantification of migration assays in b–d and f–h respectively. (n = 25, mean ± SD, *P < 0.0001, Student’s t-test). (j–k) Robust migration (white arrows) of cells from sps explants (j)

and GE explants (k) when cultured on pial ecs (j) and pv ecs (k) respectively. (l) Sometimes migration of GFP+ve cells on pv ecs recapitulated *in vivo* situation. (m–o) Migration of GFP+ve cells from GE explants when cultured with pv ecs within 6 hrs. Dotted rectangles from ‘m’ have been highlighted in ‘n’ & ‘o’ as co-labeled images. White arrows (n, o) indicate close contact of migratory cells with pv ecs. (p–u) Disruption of pv network (yellow stars, q) resulted in significant reduction of SVZ stream (yellow arrow, q) when compared to the respective control (p) while the MZ stream was unaffected (q) and disruption of pial network (green arrows, t) resulted in significant reduction of the MZ stream (yellow arrow, t) while the SVZ stream was unaffected (t). White arrows (p, s, t) point to normal SVZ streams. Blue arrows (p, q, s) point to normal MZ stream and pink arrows (p, q, s) depicts continuous pial network. White stars (p, s, t) depict normal periventricular network. White dotted box (p, q, s, t) was the area selected for cell counts. (r & u) Quantification of GAD65-GFP+ve cells in control and disrupted pv (p, q) and pial (s, t) network slices (n = 25, mean ± SD, *P < 0.001, Student’s t-test). (Scale bars: b, 100 μm (applies also to c, d, f–h, j–m, p, q, s, t); n, 50 μm (applies also to ‘o’)).

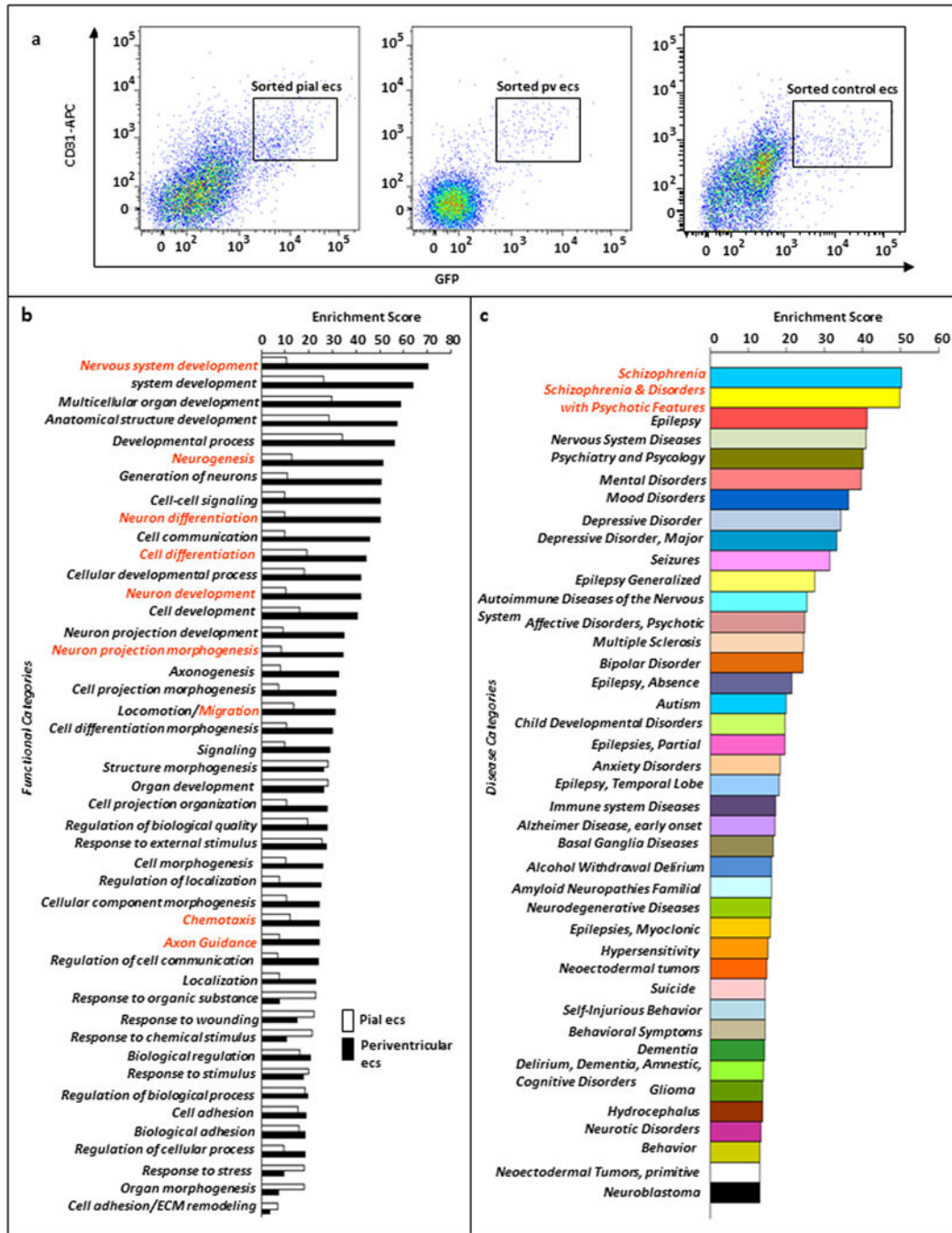


Figure 4. gene expression profile in periventricular endothelial cells and its significance for brain development and disease

(a) Dual FACS analysis of pial samples (left panel), periventricular samples (middle panel) and control samples (right panel) from E13 Tie2-GFP embryos (n=70). The purity of sorted endothelial cell samples were ensured by collection of cells that were double positive for GFP and CD-31. (b) A comparison of developmental processes' categories that were enriched in pial and periventricular endothelial cells. Some of the functional categories that represent critical developmental processes where periventricular endothelial cells might have hereto unexplored roles have been highlighted (red). (c) Periventricular angiogenesis

and disease: A classification of genes expressed in periventricular endothelial cells that were particularly enriched in several psychiatric and neurological disease categories. Schizophrenia topped the list followed closely by epilepsy.

Author Manuscript

Author Manuscript

Author Manuscript

Author Manuscript

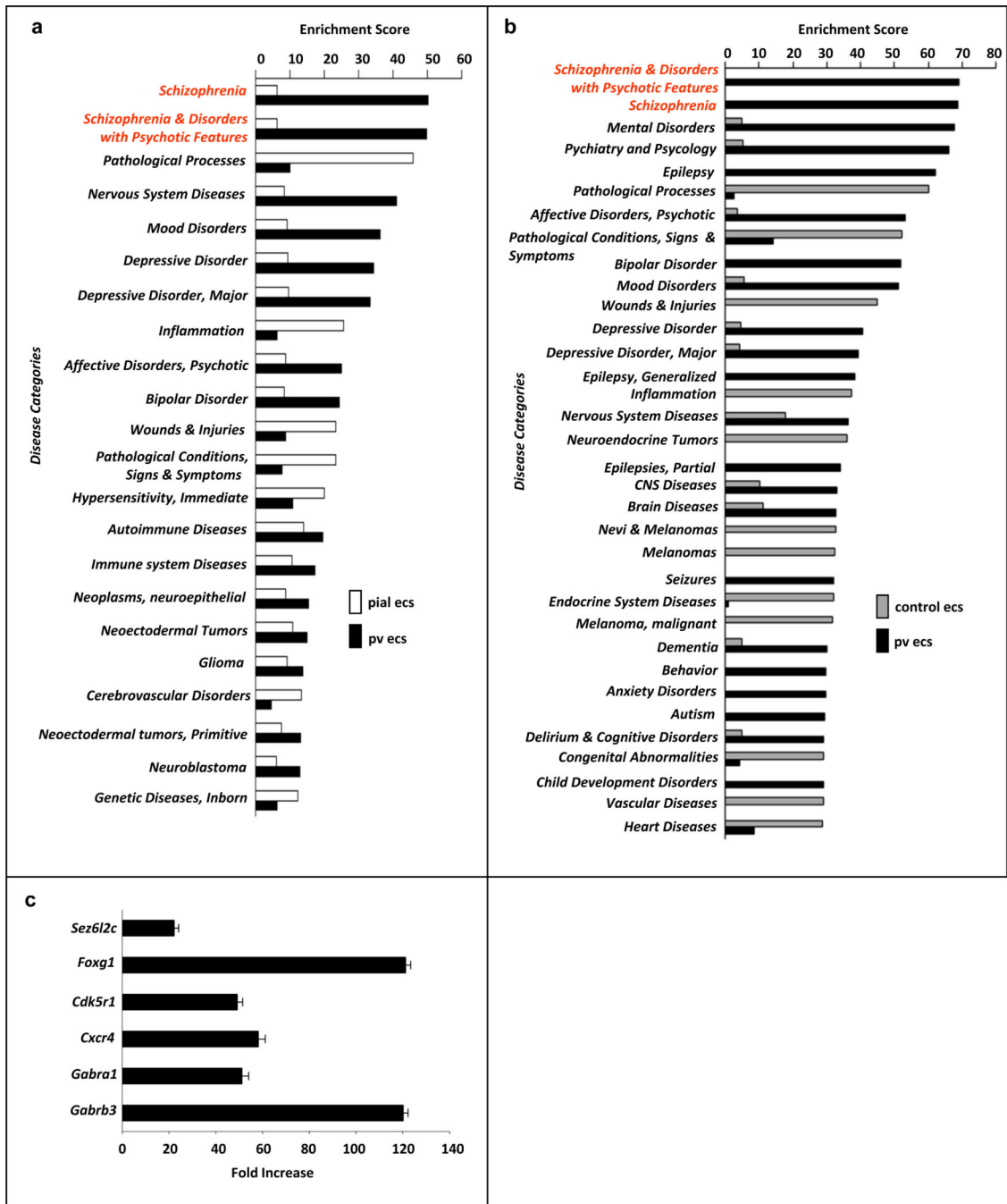


Figure 5. Periventricular angiogenesis and disease

(a) A classification of disease categories that were enriched in pial and pv ecs. Schizophrenia (highlighted in red) topped the disease category enriched in pv ecs. (b) A classification of disease categories that were enriched in control and pv ecs. Schizophrenia (highlighted in red) topped the disease category enriched in pv ecs. (c) A subset of genes believed to be expressed/traditionally confined to GABA neurons, interneurons and their precursors that were enriched in pv ecs when compared to pial ecs in the microarray screen were validated by quantitative real-time PCR (mean \pm SD).

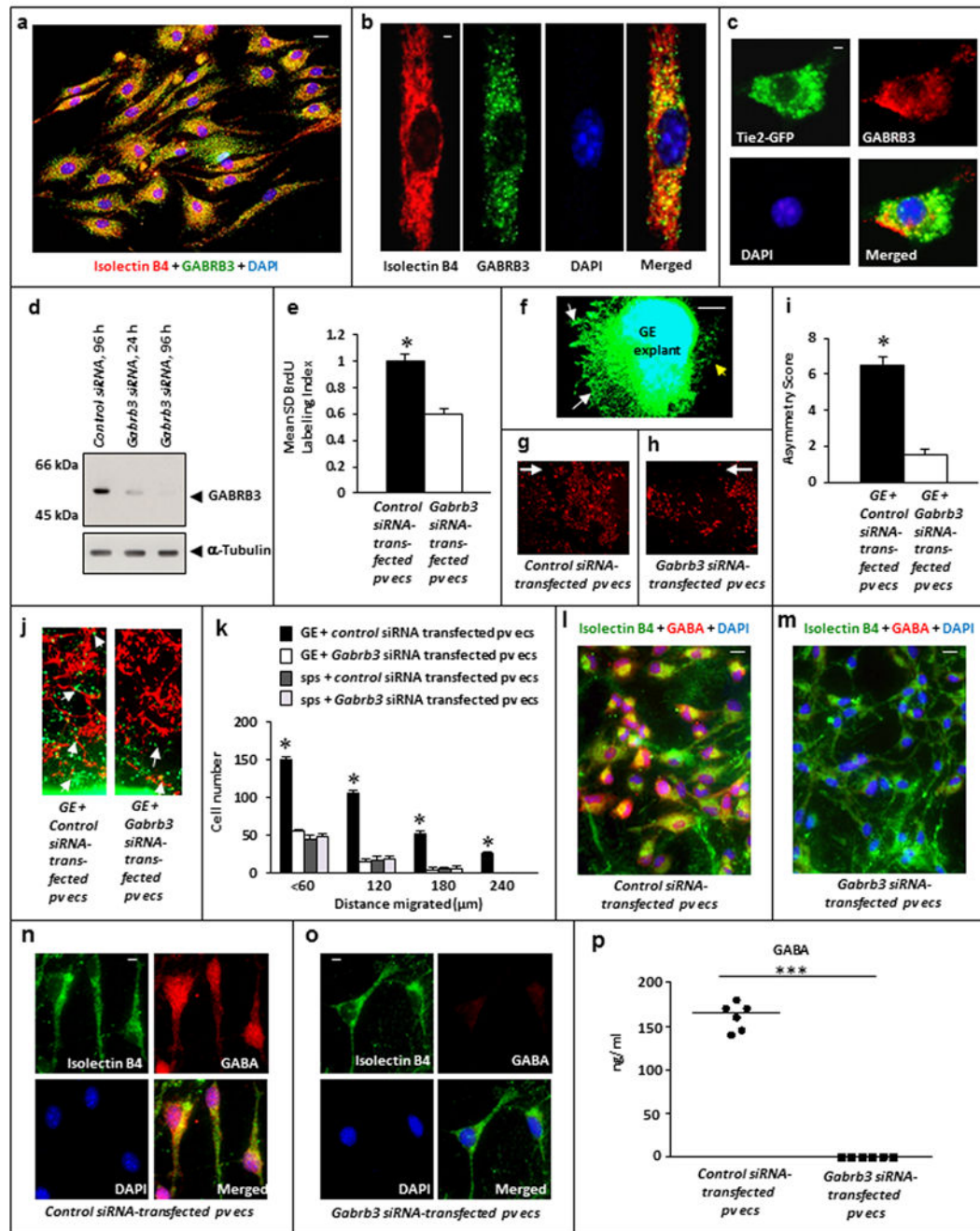


Figure 6. Autonomous roles of GABA_A receptors in periventricular angiogenesis that influences deep GABA neuron populations

(a) A low magnification co-labeled image of isolectin B4, GABRB3 and DAPI labeling of pv ecs. (b) Individual isolectin B4, GABRB3, DAPI and co-labeled image of a pv ec (60x). (c) GFP, GABRB3, DAPI and merged image of a pv ec from Tie2-GFP telencephalon (40x). (d) Virtually complete knockdown of GABRB3 in pv ecs after 96 hrs of *Gabrb3* siRNA-transfection versus control transfections. α -tubulin was used as a loading control. (e) BrdU labeling indices were significantly decreased (n=20, mean \pm SD, *P < 0.001, Student's t-

test) in *Gabrb3* siRNA-transfected pv ecs when compared to control siRNA-transfected pv ecs. (f) GE explants showed marked chemoattraction (white arrows) to control siRNA-transfected pv ecs and this chemoattractive activity was significantly reduced (yellow arrow) towards *Gabrb3* siRNA transfected pv ecs. (g–h) Migration of control (g) and *Gabrb3* (h) siRNA-transfected pv ecs towards GE explant. Arrows show direction of ecs migration towards explant. (i) Quantification of attraction of GE cells towards control and *Gabrb3* siRNA-transfected pv ecs ($n = 25$, mean \pm SD, * $P < 0.001$, Student's t-test). (j) Cell migration from GE explants was significantly decreased when cultured on *Gabrb3* siRNA-transfected pv ecs when compared to control siRNA-transfected pv ecs. White arrows point to cell migration from explant. (k) Quantification of migration assays of GE and sps explants on control and *Gabrb3* siRNA-transfected pv ecs. Plot shows average \pm SD ($n = 20$, * $P < 0.0001$, Student's t-test, group 'GE + control siRNA-transfected pv ecs' compared to group 'GE + *Gabrb3* siRNA-transfected pv ecs'). (l–m) Co-labeled images of isolectin B4, GABA and DAPI labeling of control (l) and *Gabrb3* (m) siRNA-transfected pv ecs after 96 hrs. (n–o) Individual isolectin B4, GABA and DAPI labeling of control (n) and *Gabrb3* (o) siRNA-transfected pv ecs and merged images at 60x magnification. (p) *Gabrb3* siRNA-transfected pv ecs failed to secrete GABA in contrast to control siRNA-transfected pv ecs ($n = 6$, mean \pm SD, *** $P < 0.001$, Student's t-test). Scale bar: a, 50 μm (applies also to l, m); b, 15 μm (applies also to c, n, o); f, 100 μm (applies to g, h, j).

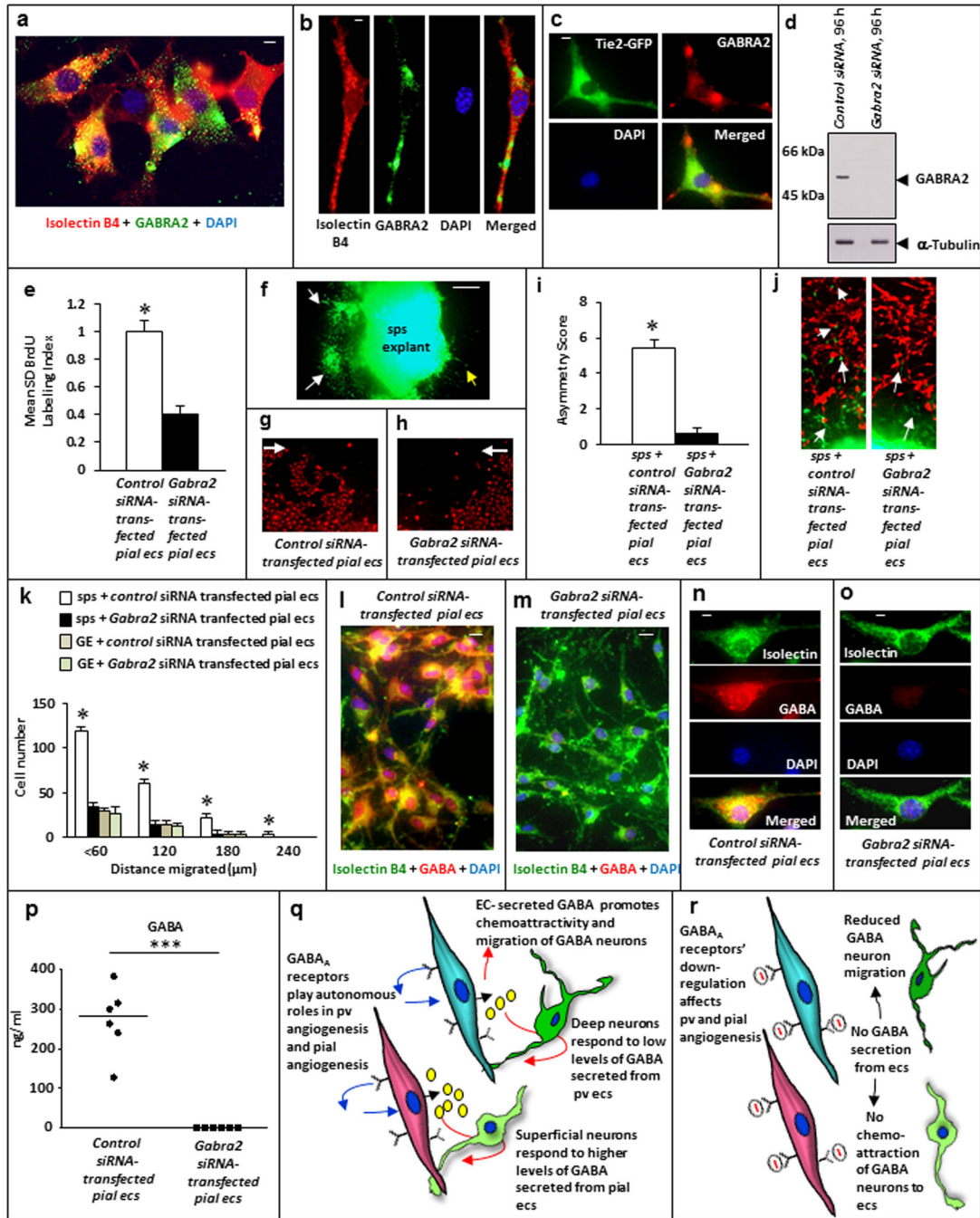


Figure 7. Autonomous roles of GABA_A receptors in pial angiogenesis that influences superficial GABA neuron populations

(a–b) A low magnification co-labeled image of isolectin B4, GABRA2 and DAPI labeling of pial ecs. (b) Isolectin B4, GABRA2 and DAPI labeling of a pial ec (48x). (c) GFP, GABRA2 and DAPI labeling of a pial ec (23x). (d) Complete knockdown of GABRA2 in pial ecs after 96 hrs of *Gabra2* siRNA-transfection versus control transfections. α -tubulin was used as loading control. (e) BrdU labeling indices were significantly decreased in *Gabra2* siRNA-transfected pial ecs (n=20, mean \pm SD, *P < 0.001, Student’s t-test). (f) sps

explants showed chemoattraction (white arrows) to control siRNA-transfected pial ecs and this chemoattraction was reduced (yellow arrow) towards *Gabra2* siRNA-transfected pial ecs. (g–h) Migration of control (g) and *Gabra2* (h) siRNA-transfected pial ecs towards sps explant. Arrows show direction of migration. (i) Quantification of sps explant chemoattraction towards control and *Gabra2* siRNA-transfected pial ecs (n = 25, mean ± SD, *P < 0.0001, Student's t-test). (j) Cell migration from sps explants was decreased when cultured on *Gabra2* siRNA-transfected pial ecs. White arrows illustrate cell migration. (k) Quantification of migration assays of GE and sps explants on control and *Gabra2* siRNA-transfected pial ecs (n = 20, mean ± SD, *P < 0.0001, Student's t-test, group 'sps + control siRNA-transfected pial ecs' compared to group 'sps + *Gabra2* siRNA-transfected pial ecs'). (l–m) Co-labeled images of isolectin B4, GABA and DAPI labeling of control (l) and *Gabra2* (m) siRNA-transfected pial ecs. (n–o) Individual isolectin B4, GABA and DAPI labeling of control (n) and *Gabra2* (o) siRNA-transfected pial ecs (60x). (p) *Gabra2* siRNA-transfected pial ecs failed to secrete GABA in contrast to control siRNA-transfected pial ecs (n = 6, mean ± SD, ***P < 0.001, Student's t-test) (q–r) Schema of GABA_A receptors-GABA signaling in pv ecs (blue) and pial ecs (pink) that has consequences for deep (dark green) and superficial (light green) GABA neuron populations. GABA_A receptors depicted as black 'Y' and GABA as yellow circles. Scale bar: a, 40 μm; b, 13 μm; c, 28 μm, f, 100 μm (applies to g, h, j); l, 50 μm (applies also to m); n, 15 μm (applies also to o).